Supporting Information

Blowing-Inspired *Ex-Situ* Preparation of Ultrathin Hydrogel Coatings for Visibly Monitoring Humidity and Alkaline Gas

Xiao He,[1] Ruijie Yang,[1] Chaochen Xu,[2] Ziqian Zhao,[3] Y. Frank Cheng,[2] Philip Egberts,[2] Hongbo Zeng,[3] and Qingye Lu [1*]*

[1] Department of Chemical and Petroleum Engineering, University of Calgary, Calgary, Alberta T2N 1N4, Canada

[2] Department of Mechanical and Manufacturing Engineering, University of Calgary, Calgary, Alberta T2N 1N4, Canada

[3] Department of Chemical & Materials Engineering, University of Alberta, Edmonton, Alberta T6G 1H9, Canada

[*]Corresponding author：E-mail: hongbo.zeng@ualberta.ca (H. Zeng); qingye.lu@ucalgary.ca (Q. Lu)

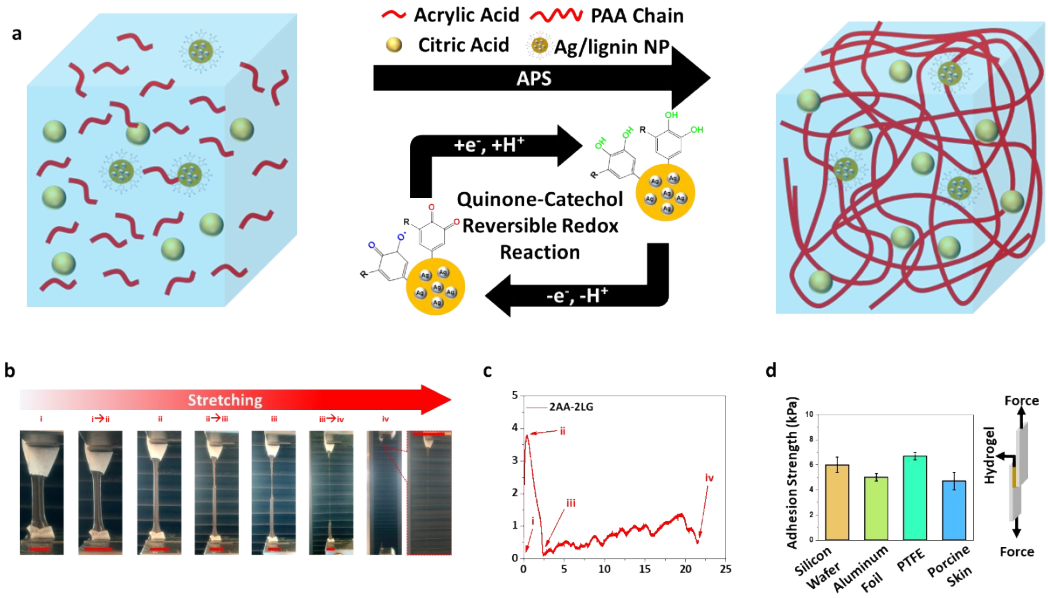

Fig. S1. Gelation mechanism and characterization of PAA hydrogel based on the quinone/semiquinone-catechol redox system by Ag/lignin NPs. a) Schematic illustration of gelation process of PAA hydrogel. b) Necking behavior of 2AA-2LG hydrogel during the stretching process. c) Tensile stress-curve of 2AA-2LG hydrogel during stretching, the peak of the curve indicates the presence of necking behavior. d) Adhesion strength of 2AA-2LG hydrogel on different substrates (silicon wafer: 6.0±0.6 kPa, aluminum foil: 5.0±0.3 kPa, PTFE: 6.7±0.3 kPa and porcine skin: 4.7±0.7 kPa). The scale bar in Fig. S1b is 1 cm.

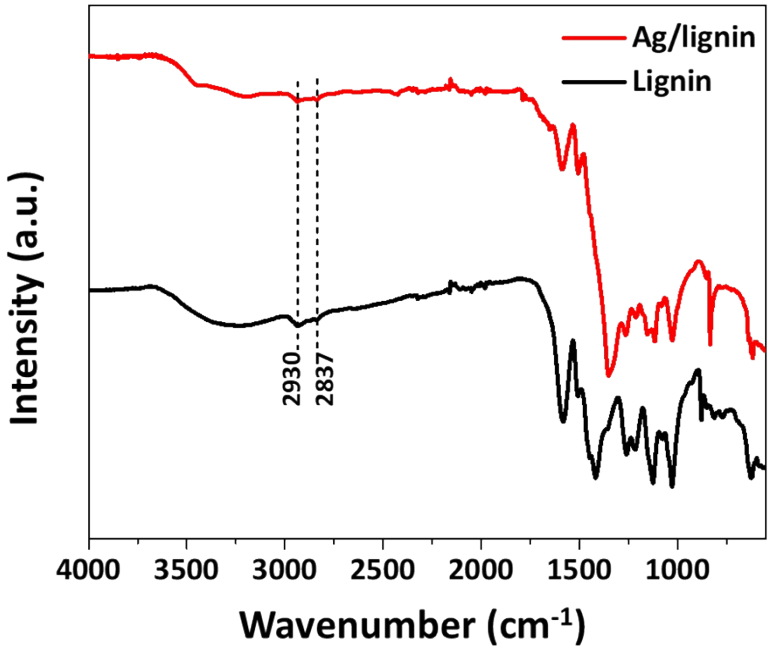

Fig. S2. FT-IR spectra of Ag/lignin NPs and lignin. The peak at 2837 cm^{-1} stands for -CH_3 in the methoxy groups and the peak at 2930 cm^{-1} is assigned to methyl and methylene groups,[1] suggesting the partial hydrophobicity of lignin and Ag/lignin NP surfaces.

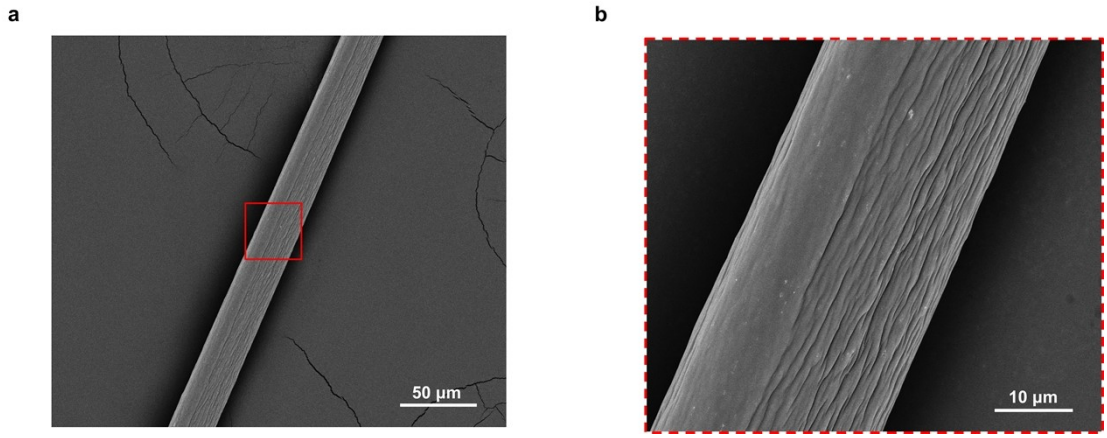

Fig. S3. SEM image of a hydrogel fiber generated by extending the 2AA-2LG hydrogel after necking propagation. Fig. S3b is the enlarged view of area shown in the read box in Fig. S3a.

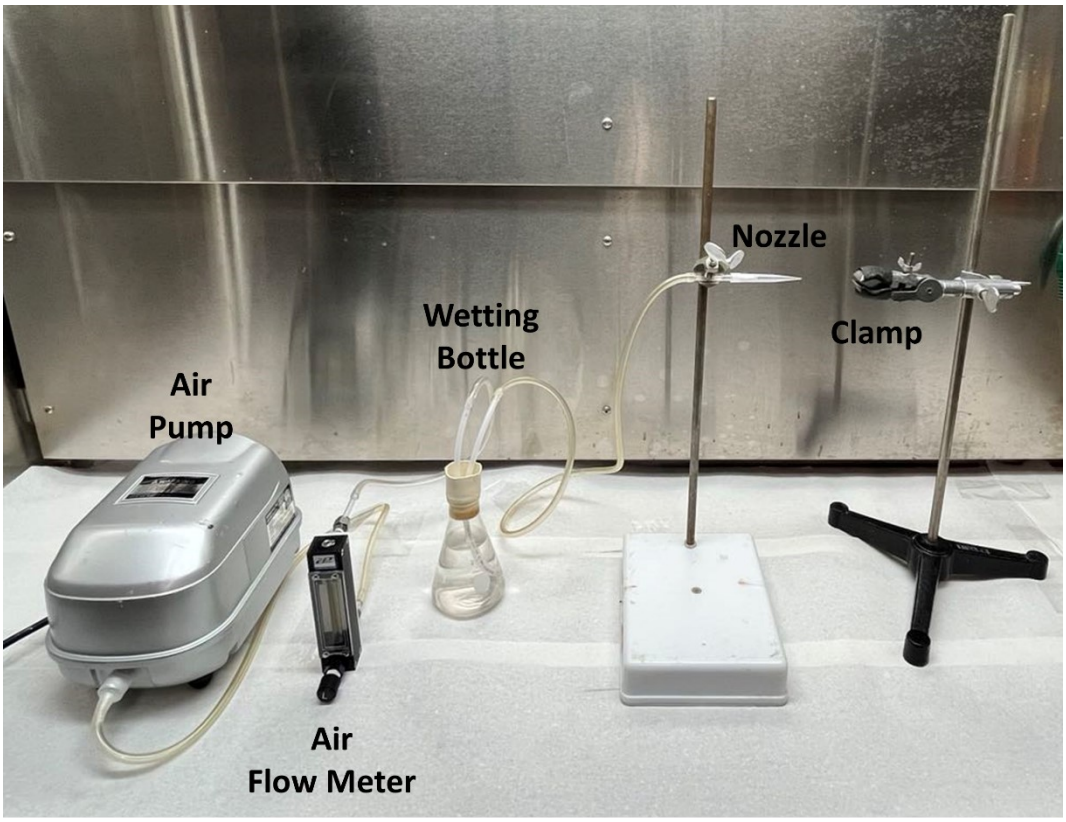

Fig. S4. House-built apparatus to fabricate hydrogel coatings using bubble blowing strategy.

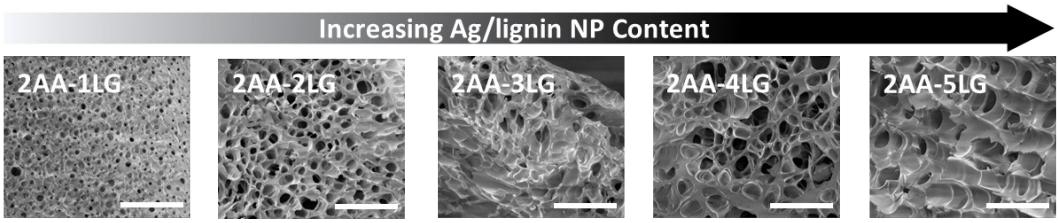

Fig. S5. Porous structures of hydrogels with different contents of Ag/lignin particles by SEM imaging, indicating that a higher content of Ag/lignin NPs resulted in a less compact network and larger pore sizes. The scale bars are 100 μm.

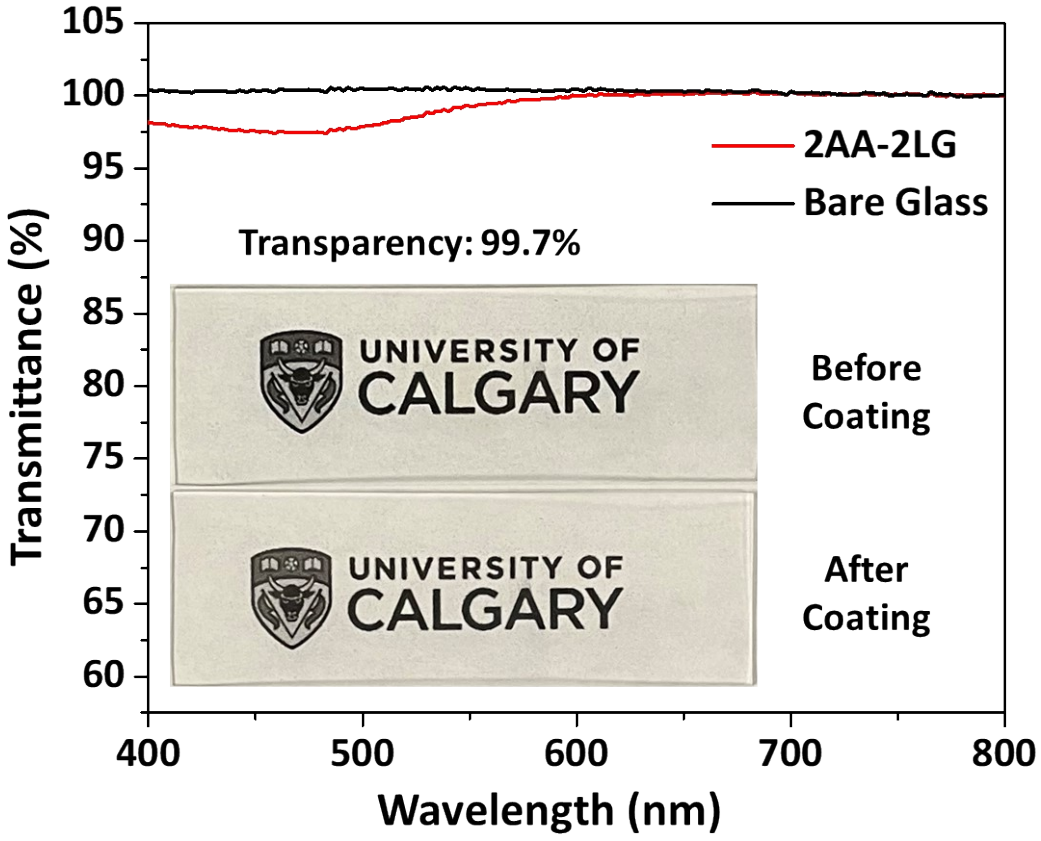

Fig. S6. High transparency of an ultrathin hydrogel coating on a glass slide.

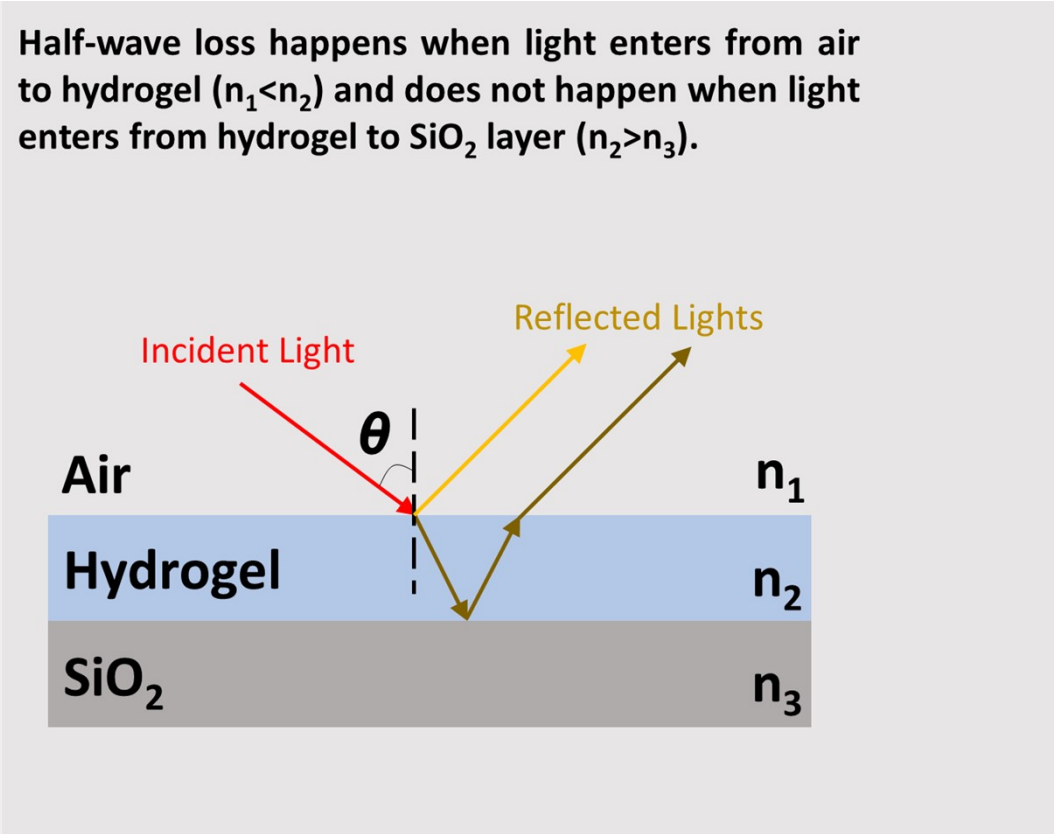

Fig. S7. Schematic interference of the two reflected light from the air-hydrogel coating and hydrogel coating-SiO_2. n_1, n_2 and n_3 are the refractive indices of air, hydrogel and SiO_2, respectively. θ is the incident angle of light.

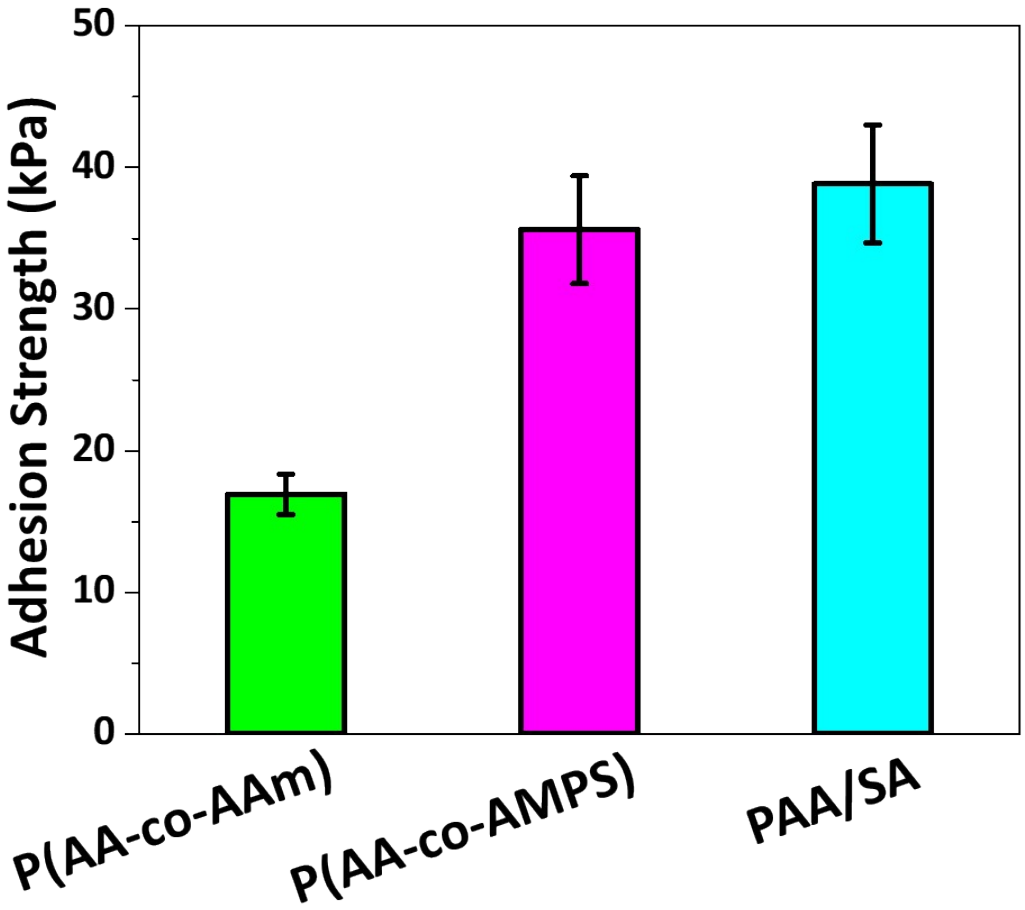

Fig. S8. Adhesive properties of PAA/SA double network hydrogel, P(AA-*co*-AAm) hydrogel and P(AA-*co*-AMPS) hydrogel gelated *via* dynamic quinone-catechol redox system by Ag/lignin NPs onto silicon wafer, favoring the transferring of the hydrogel films to the wafer surface (P(AA-co-AAm): 16.9±1.4 kPa, P(AA-co-AMPS): 35.6±3.8 kPa, PAA/SA: 38.8±4.1 kPa).

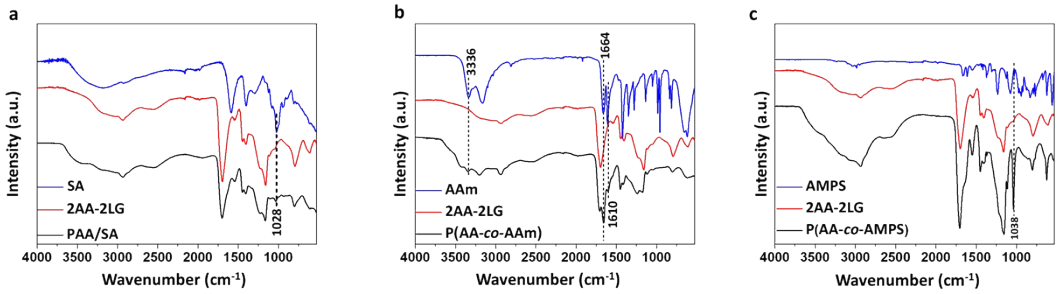

Fig. S9. FT-IR spectra of different coatings fabricated using bubble blowing strategy using a) PAA/SA DN hydrogel, b) P(AA-*co*-AAm) SN hydrogel and c) P(AA-*co*-AMPS) SN hydrogel on silicon wafers. Fig. a: peak at 1028 cm^{-1} represents the stretching vibration of –C-OH of sodium alginate;[2] Fig. b: peaks at 3336 cm^{-1}, 1664 cm^{-1}, and 1610 cm^{-1} represents the N-H stretching, C=O stretching and C-C stretching of acrylamide, respectively;[3] Fig. c: peak at 1038 cm^{-1} represents the sulfonic groups of AMPS.[4]

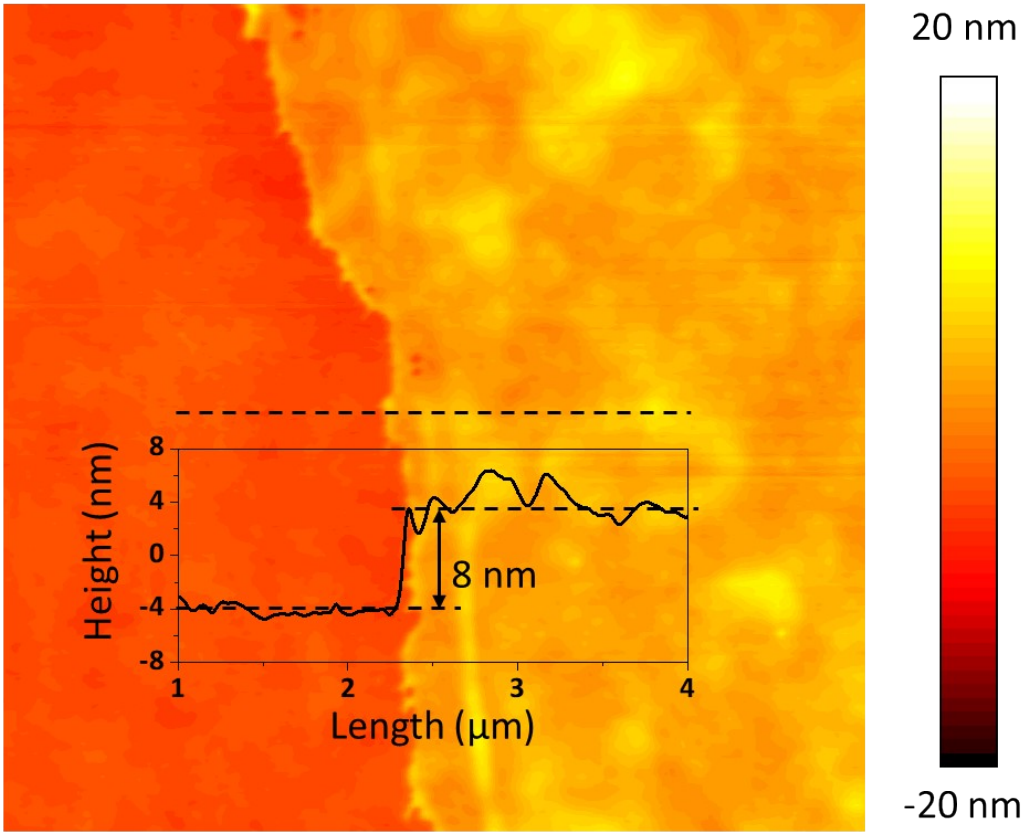

Fig. S10. AFM image (5×5 µm) of edge area of the PAA/SA hydrogel coating.

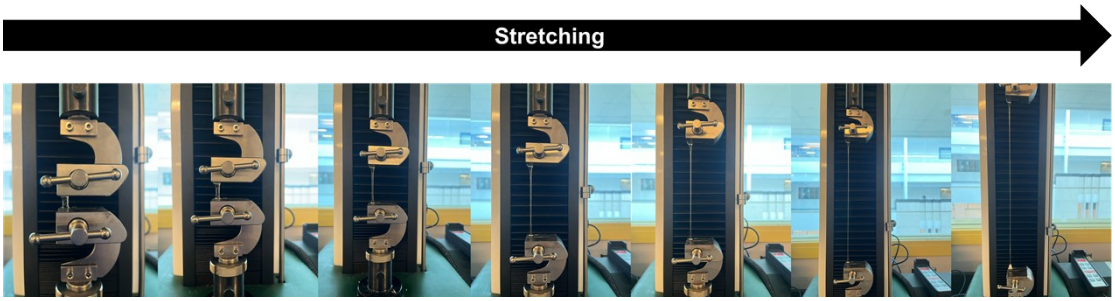

Fig. S11. Stretching pure PAA hydrogel prepared using APS under the external stimulus of thermal and no obvious necking behavior was observed.

Fig. S12. Necking propagation of PAA+1LG hydrogel containing a proper amount of lignin particles, indicating that the addition of lignin particles would lead to the necking behavior of hydrogel.

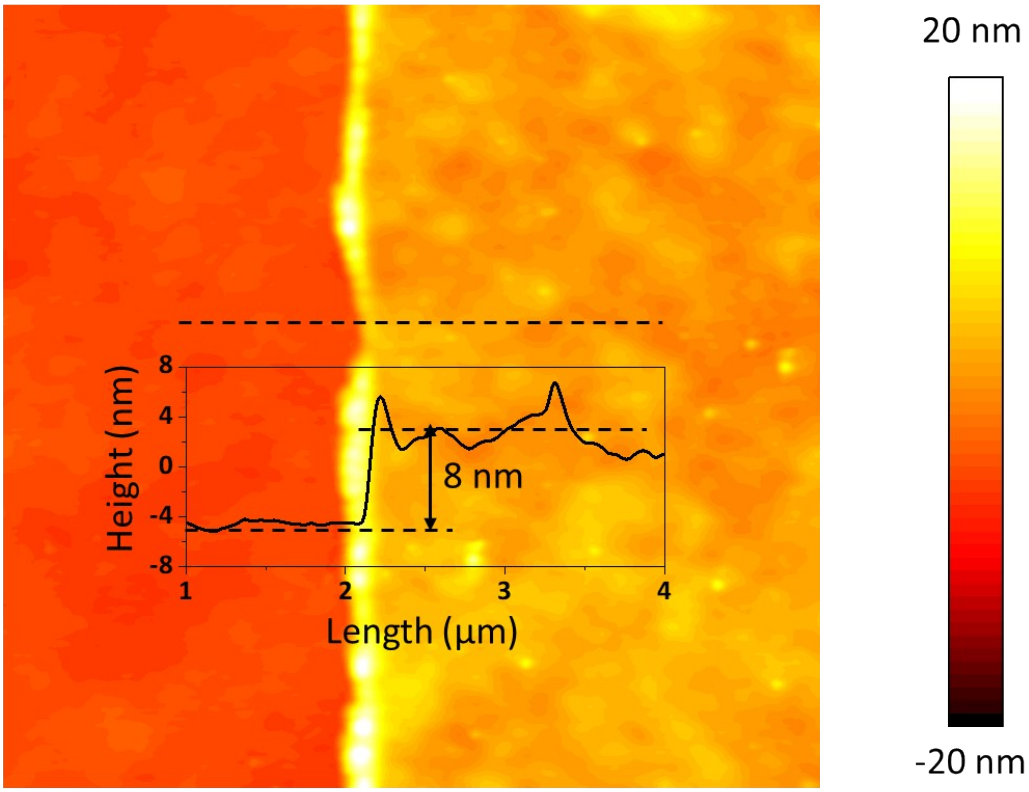

Fig. S13. AFM image (5×5 μm) of edge area of the PAA+3LG hydrogel coating.

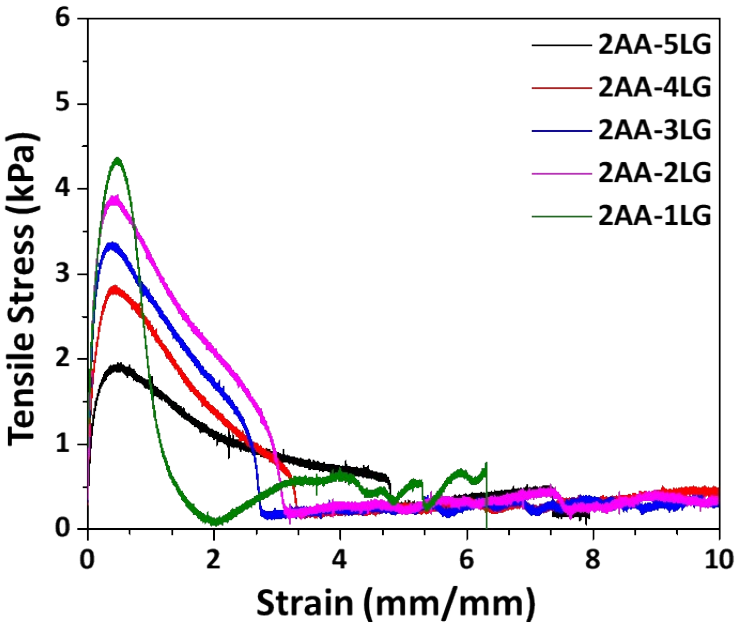

Fig. S14. The tensile stress-strain curves of hydrogels containing different contents of Ag/lignin NPs.

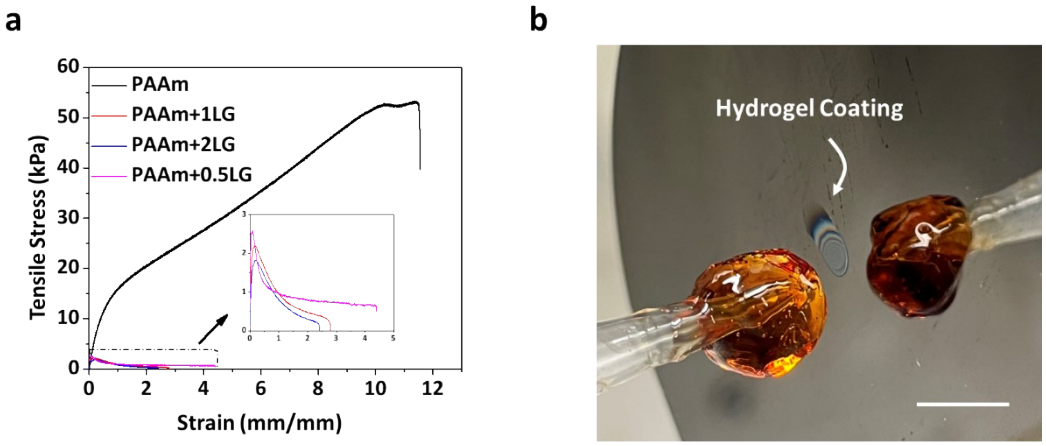

Fig. S15. a) Mechanical properties of PAAm hydrogels with or without the presence of lignin particles, demonstrating that the addition of lignin particles into hydrogel could lead to obvious necking behavior. b) A hydrogel coating on silicon wafer prepared using PAAm+0.5 LG hydrogel *via* bubble blowing strategy, the near transparent part of coating near the edge area suggests the ultrathin thickness. The scale bars are 1 cm.

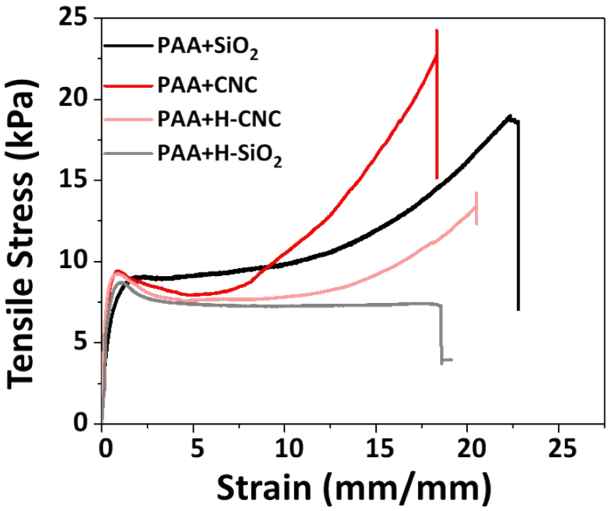

Fig. S16. Mechanical properties of PAA hydrogels containing hydrophilic particles (SiO_2 and CNC) or hydrophobized particles (H-SiO_2 and H-CNC).

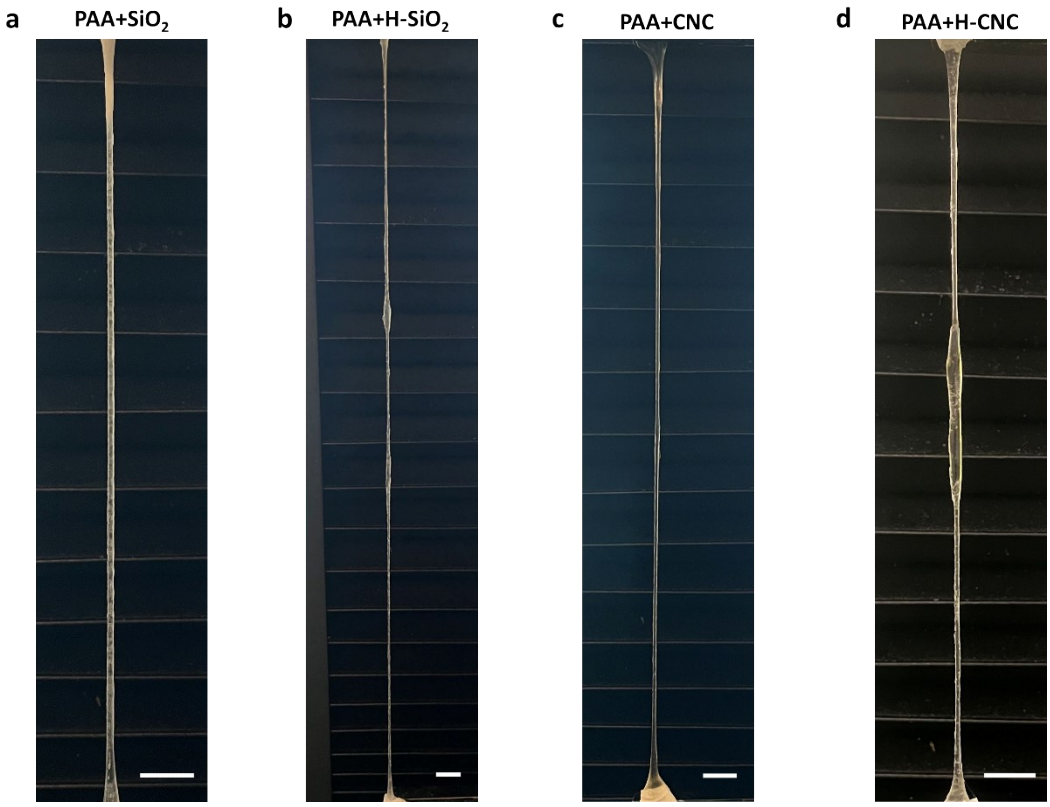

Fig. S17. Stretching process of a) PAA+SiO_2 NP hydrogel, b) PAA+H-SiO_2 NP hydrogel, c) PAA+CNC hydrogel and d) PAA+H-CNC hydrogel, demonstrating the benefit of hydrophobic particles on the mobility of polymer chains and resulting necking behavior during stretching process. The scale bars are 1 cm.

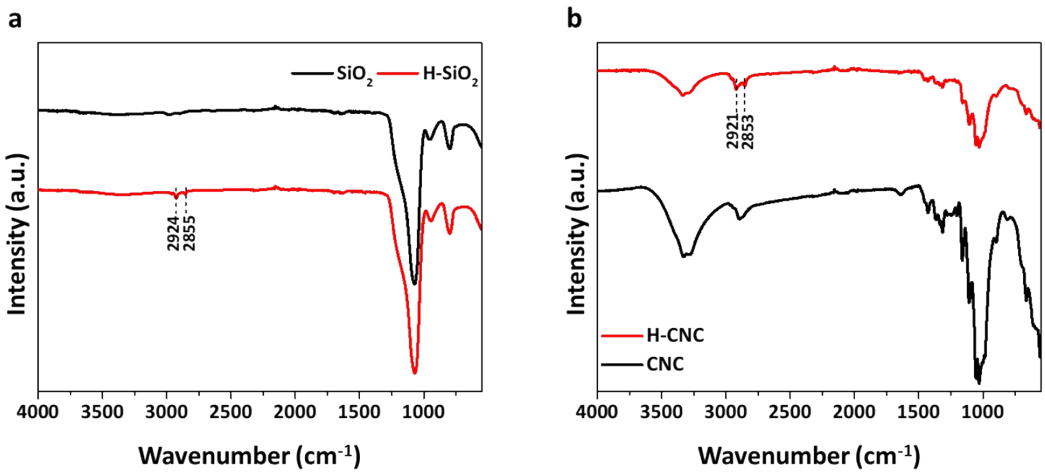

Fig. S18. FT-IR spectrum of a) SiO_2 and b) CNC with or without hydrophobization. The peaks at ~2924 and ~2855 cm^{-1} of H-SiO_2, and ~2921 and 2853 cm^{-1} stand for the C–H asymmetric and symmetric stretching vibration in all hydrocarbon constituents,[5] suggesting the grafting of hydrophobic functional groups.

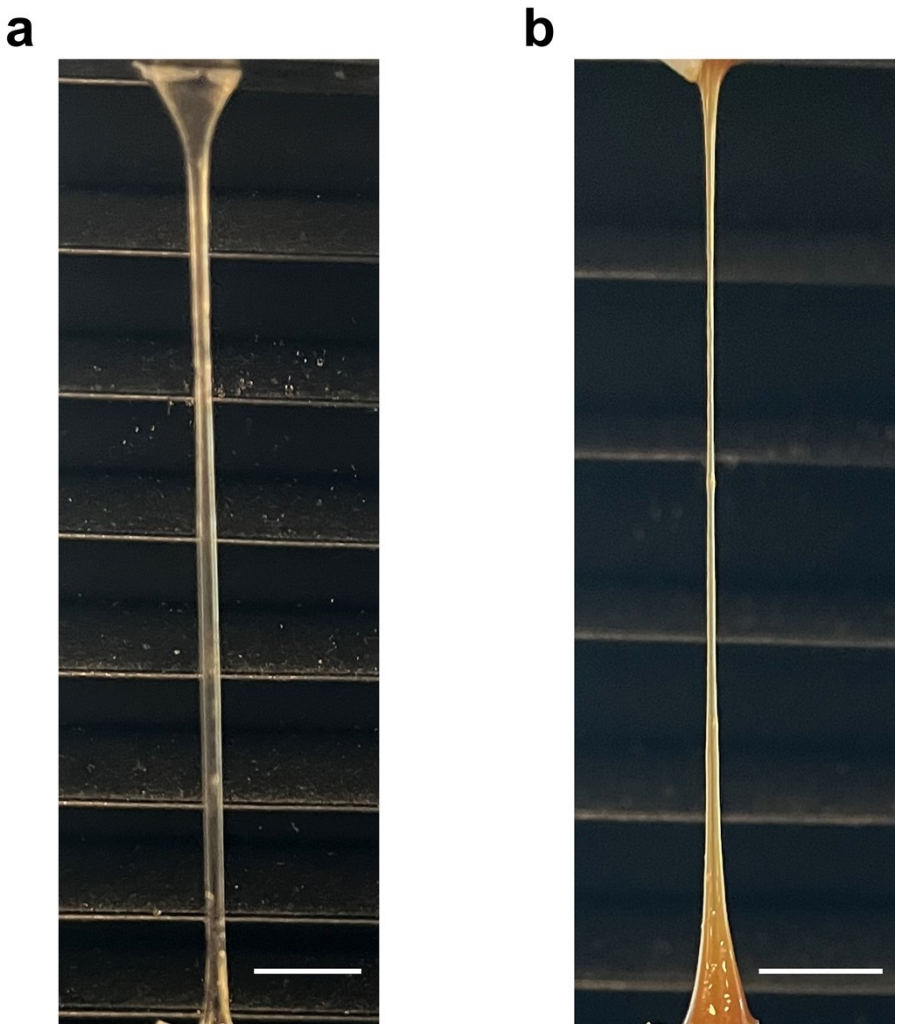

Fig. S19. Stretching of a) PAA+0.001MBAA hydrogel and b) PAA+0.001MBAA+3LG, indicating the necking behavior of the hydrogel after adding lignin particles. The scale bars are 1 cm.

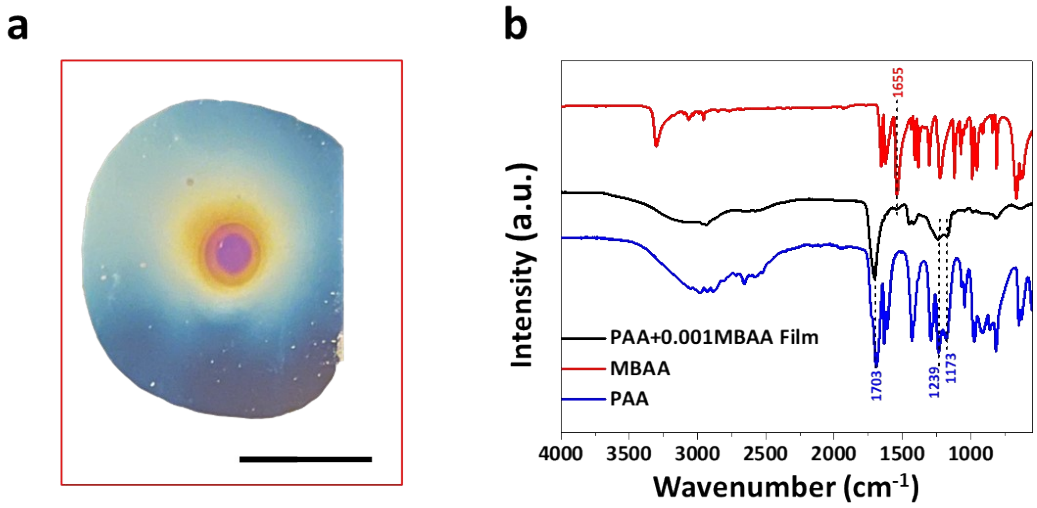

Fig. S20. a)Hydrogel coating fabricated using PAA+0.001MBAA hydrogel and b) FT-IR spectra of ultrathin hydrogel film fabricated using PAA+0.001MBAA hydrogel *via* blowing strategy. MBAA: 1655 cm^{-1}: C=O stretching; PAA: 1703 cm^{-1}: C-O vibration, 1239 cm^{-1}: C-O stretching coupled with O-H in-plane bending mode, 1173 cm^{-1}: C-O stretching of neighboring carboxyl groups. The scale bar is 1 cm.

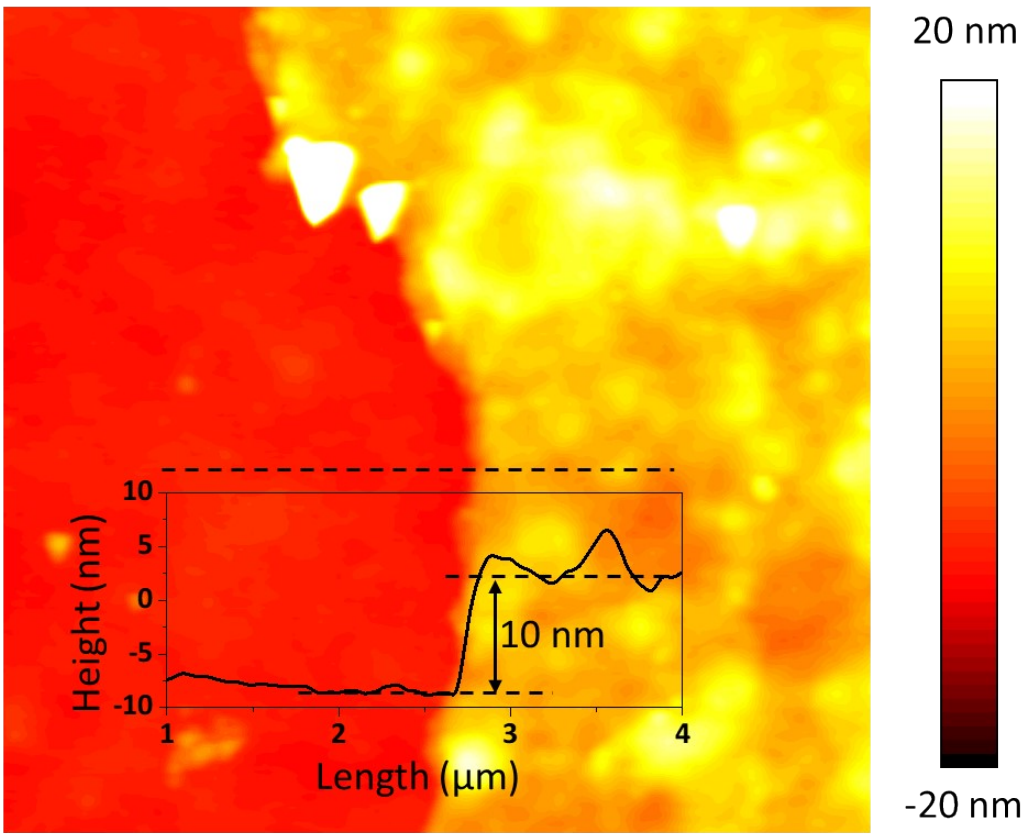

Fig. S21. AFM image (5×5 μm) of edge area of the PAA+0.001MBAA+3LG hydrogel coating.

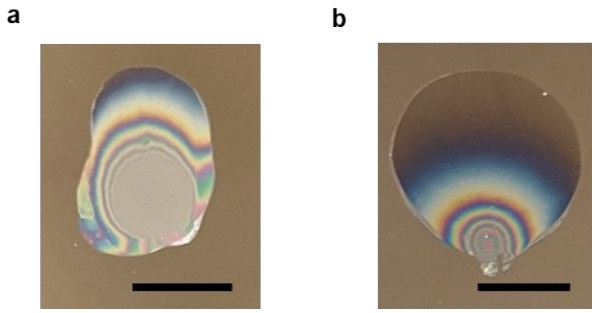

Fig. S22. Ultrathin hydrogel coatings prepared *via* blowing strategy using a) PAA+0.1 MBAA+3LG and b) PAA+0.01MBAA+3LG, respectively, and the near-transparency of the coating around edge area suggests the ultrathin thickness of the coating. The tensile stress-strain curves of the corresponding hydrogels are shown in Fig. 4f. The scale bars are 1 cm.

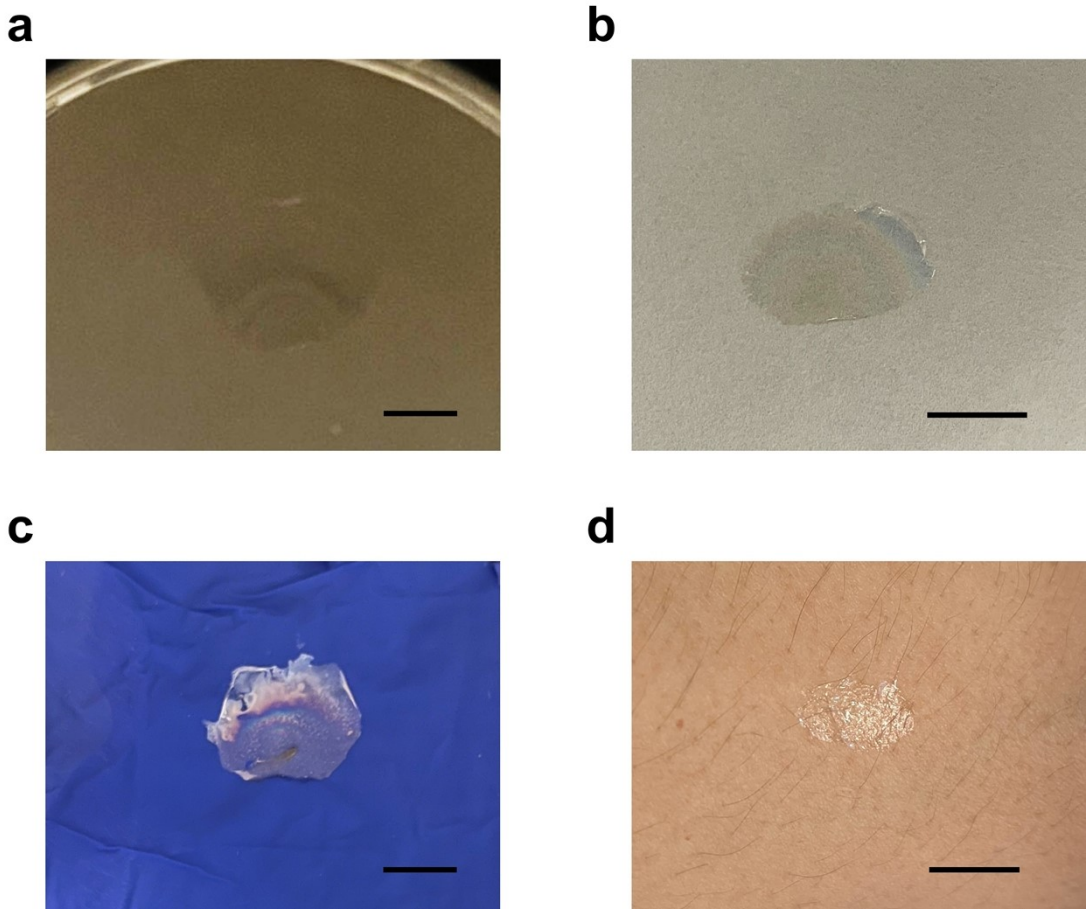

Fig. S23. Fabrication of 2AA-2LG hydrogel film using blowing strategy onto different substrates: a) PTFE, b) filter paper, c) rubber glove and d) human skin. The scale bars in Fig.s are 1 cm.

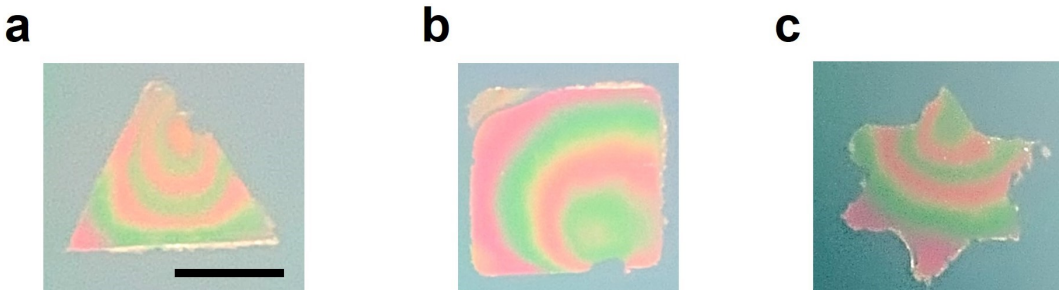

Fig. S24. Fabrication of 2AA-2LA hydrogel films with masking method into different shapes: a) triangle, b) square and c) hexagon onto silicon wafer. The scale bar in Fig. S24a is 1 cm.

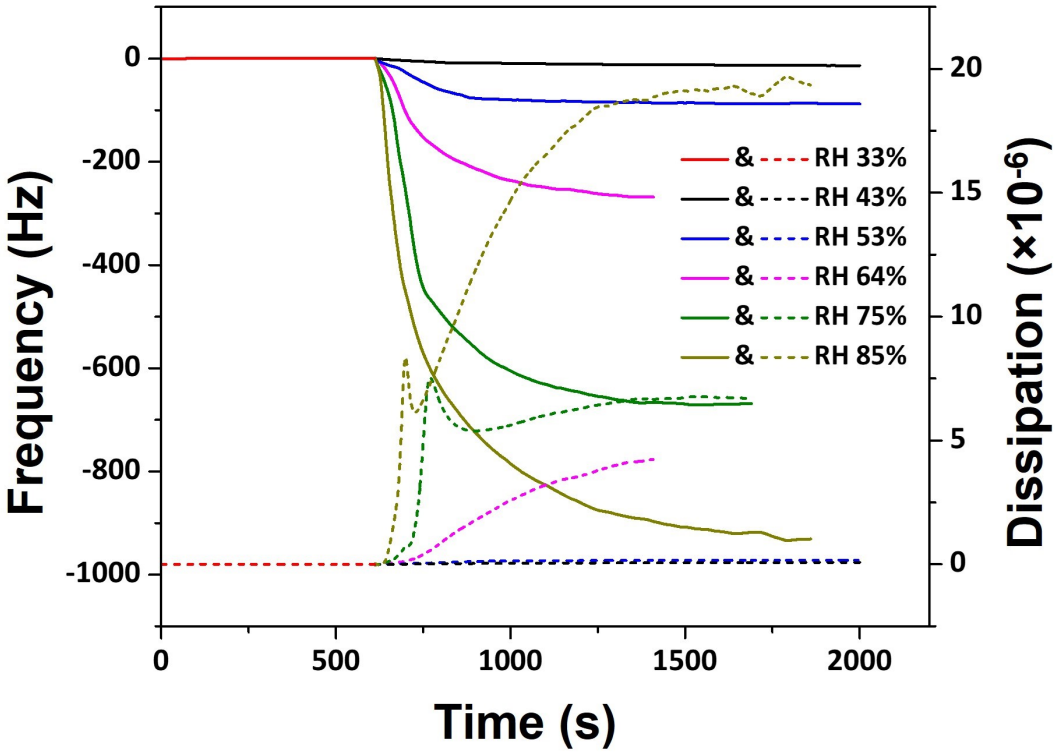

Fig. S25 The change of frequency (solid lines) and dissipation (short dash lines) of a hydrogel coating on QCM-D sensor surface (fabricated at RH 33%) in ambient environments with different humidity levels. Red: RH 33%, black: RH 44%, blue: RH 53%, pink: RH 64%, green: RH 75% and dark yellow: RH 85%. The peaks observed in the dissipation change may result from the structural change due to too much adsorbed water in hydrogel coating.

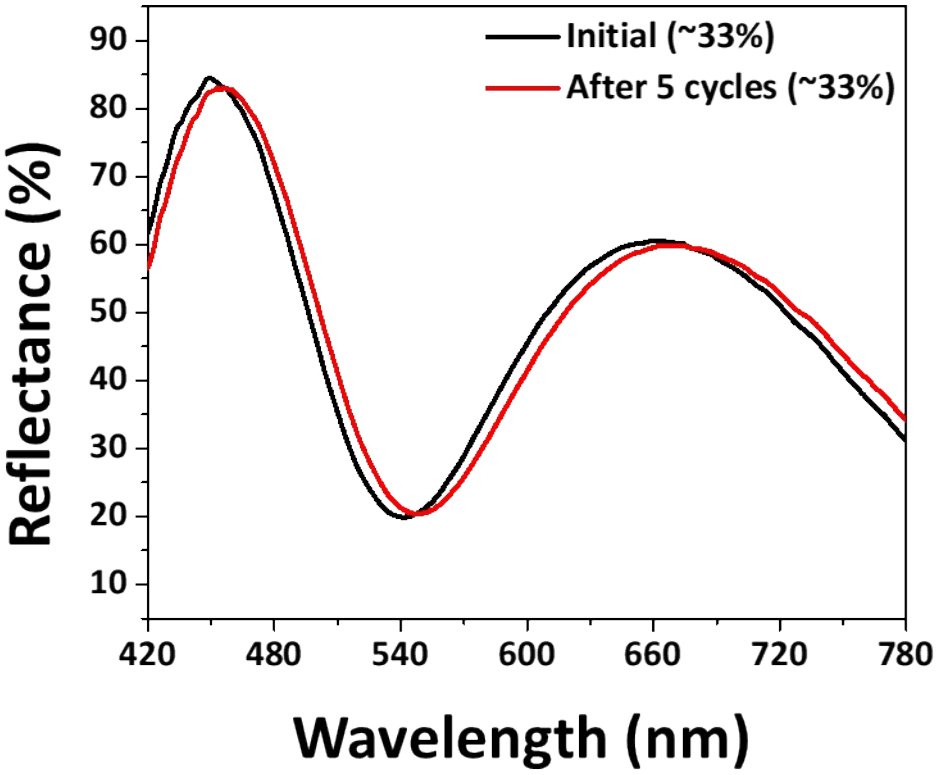

Fig. S26. The reflected spectra of the hydrogel coating after five cycles of swelling/deswelling by adsorbing/desorbing water from the ambient atmosphere. The spectra were collected from the white dot area shown in Fig. 5a and measured under an ambient condition of humidity ~33%,

Table S1. Polymer/Nanoparticle films/coatings fabricated by blowing polymer-dissolved solutions or nanoparticle suspensions.

Materials for Coating	Thickness	Preparation Method[a]	Application	Ref.
Epoxy solution	200-500 nm	Blowing+solvent evaporation	Nanorod alignment	6
Silk Solution	> 150 nm	Blowing+solvent evaporation	Soft electronics	7
TPE solution	> 90 nm	Blowing+solvent evaporation	Nano-membrane	8
GO suspension	>14.7 nm	Blowing+solvent evaporation	Conductive film	9

[a] Unlike the hydrogel coating proposed in this work, the solvent evaporation is a necessary step for the listed methods to transfer liquid films to solid or quasi-solid film.

Table S2. Comparison between the hydrogel coating fabricated using blowing strategy and the hydrogel coatings reported.

Materials for Coating	Thickness	Preparation Method [a]	Ref.
Pre-gelated hydrogels	> 5 nm	Blowing strategy	This work
NSD-Gel	> 800 μm	Flaying from goat+nanoengineering	[10]
PVA hydrogel	0.5-600 μm	Cryo-microtomy	[11]
Bacterial hydrogel	4-10 μm	Mechanical exfoliation	[12]
P(SA-*co*-AAc) dissolved-solution	40-80 μm	Solvent spreading+solvent evaporation	[13]
P2VP precursor solution	20-100 nm	Spin-coating+chemical crosslinking	[14]
PAAm/SA-Ca^{2+} hydrogel	> 20 μm	Renatured hydrogel painting	[15]
PEGDA precursor solution	~ 158 ± 16 nm	Antigen-specific coating+LED	[16]
P(AMSA-*co*-AA) precursor solution	~300 nm to 3.5 μm	Spin-coating+UV	[17]
PDMAA precursor solution	~10 μm	Submerging+UV	[18]
PDMS precursor solution	5-25 μm	Submerging+UV	[19]
PVPON/PMAA polymer solution	> 43 nm	Submerging+solvent evaporation	[20]
SA precursor solution	~ 100 nm	LbL submerging+ion crosslinking	[21]
SA precursor solution	> 3 nm	LbL submerging+ion crosslinking	[22]
PEDGA precursor solution	> 20 nm	Submerging+UV	[23]
HPMA precursor solution	> 65 nm	Submerging+UV	[24]
Cellulose precursor solution	170 ± 7 nm	Spin-coating+chemical crosslinking	[25]
PNIPAAm precursor solution	60 ± 9.2 μm	Casting+ chemical crosslinking	[26]
PVA solution	~ 20 μm	Casting+freeze-thawing	[27]

Fe^{3+}-PAA precursor solution	~ 2mm	Casting+crosslinking	[28]
CS/PEG precursor solution	~ 150 nm	Submering+chemical crosslinking	[29]
P(HEMA-*co*-AAc) precursor solution	> 100 nm	Spin-coating+UV	[30]
P(AAm-*co*-AAc-*co*-AAene) precursor solution	~ 300 nm	Spin-coating+UV	[31]
P(NIPAm-co-TMSPMA) precursor solution	2-20 μm	Dipping/Brushing/Spraying+UV	[32]
PVA/TA precursor solution	~ 1.9 μm	Dipping/Brushing/Spraying+solvent evaporation	[33]
PEG-ACLT precursor solution	~7 μm	Spraying+UV	[34]
PAA precursor solution	~ 600 nm	Submerging+UV-	[35]
P(CBAA) precursor solution	15-150 nm	Submerging+chemical crosslinking	[36]
PVA precursor solution	> 30 nm	Dip-coating+chemical crosslinking	[37]
PVA/Salicylic Acid	~120 nm	Spin-coating+freeze-thawing	[38]
ALG/CHI/HA precursor solution	~71 nm	LbL submerging +chemical crosslinking	[39]
PAAm precursor solution	> 2 μm	Molding+UV	[40]
PAAm+alginate precursor solution	> 7 μm	Cold-lamination+UV	[41]
PNIAAm+CS precursor solution	~500 μm	Submerging+UV	[42]
PDMS precursor solution	> 12.15μm	LbL spin-coating+thermal	[43]

[a] For the preparation method, *ex-situ* methods are highlighted in grey, which refer to coating of already-gelated hydrogels. *In-situ* methods are highlighted in blue, which refer to locating hydrogel precursor solution on targeting surface, followed by curing step to obtain final hydrogel coating.

Table S3. Comparison between the thicknesses of the hydrogel coating measured using a commercial instrument Filmetrics and theoretical thicknesses calculated from wavelengths at constructive and destructive peaks in corresponding spectrum.

Measured Thickness (nm)	Theoretical Thickness (nm)
31	-
53	-
101	119
110	131
174	169
253	248
291	266
344	314
447	418

Table S4. Preparation of Ag/lignin NP solutions with different concentrations of Ag/lignin NPs.

Lignin Aqueous Solution (2.5 mL)	**$AgNO_3$ (mg)**	**5M $NH_3 \cdot H_2O$ (mL)**	**DI Water (mL)**	**Abbreviation**
0 mg/mL	0	0.5	2	Ag/0LG NP
10 mg/mL	15.75	0.5	2	Ag/1LG NP
20 mg/mL	31.5	0.5	2	Ag/2LG NP
30 mg/mL	47.25	0.5	2	Ag/3LG NP
40 mg/mL	63	0.5	2	Ag/4LG NP
50 mg/mL	78.75	0.5	2	Ag/5LG NP

Table S5. Preparation of Ag/lignin hydrogel using different Ag/LG NP solutions.

1 wt% APS (mL)	Ag/LG NP Solution (mL)	Other Materials (mg)	AA (mL)	5 w/v% CA/Water (mL)	Abbr.
1	Ag/0LG NP, 2.5	-	2	1.5	2AA-0LG
1	Ag/1LG NP, 2.5	-	2	1.5	2AA-1LG
1	Ag/2LG NP, 2.5	-	2	1.5	2AA-2LG
1	Ag/3LG NP, 2.5	-	2	1.5	2AA-3LG
1	Ag/4LG NP, 2.5	-	2	1.5	2AA-4LG
1	Ag/5LG NP, 2.5	-	2	1.5	2AA-5LG
1	Ag/2LG NP, 2.5	-	1.5	1.5	1.5AA-2LG
1	Ag/2LG NP, 2.5	-	1	1.5	1AA-2LG
1	Ag/2LG NP, 2.5	AAm, 400	1	1.5	P(AAm-*co*-AA)
1	Ag/2LG NP, 2.5	AMPS, 400	1	1.5	P(AA-*co*-AMPS)
1	Ag/2LG NP, 2.5	SA, 400	1	1.5	PAA/SA

Table S6. Preparation of hydrogels polymerized using thermal initiator.

1 wt% APS (mL)	NP Suspension (mL)	Other Materials (mg)	AA (mL)	5 w/v% Aqueous Solution (mL)	Abbr.
1	DI water, 2.5	-	2	DI Water, 1.5	PAA
1	10 mg/mL lignin particle, 2.5	-	2	DI Water, 1.5	PAA+1LG
1	20 mg/mL lignin particle, 2.5	-	2	DI Water, 1.5	PAA+2LG
1	30 mg/mL lignin particle, 2.5	-	2	DI Water, 1.5	PAA+3LG
1	40 mg/mL lignin particle, 2.5	-	2	DI Water, 1.5	PAA+4LG
1	20 mg/mL SiO_2 NP, 2.5	-	2	5 w/v% CA/Water, 1.5	PAA+SiO_2
1	20 mg/mL TiO_2 NP, 2.5	-	2	5 w/v% CA/Water, 1.5	PAA+TiO_2
1	20 mg/mL cellulose particle, 2.5	-	2	5 w/v% CA/Water, 1.5	PAA+Cellulose
1	20 mg/mL H-SiO_2 NP, 2.5	-	2	5 w/v% CA/Water, 1.5	PAA+H-SiO_2
1	DI water, 2.5	MBAA, 4.6	2	DI Water, 1.5	PAA+0.1MBAA[a]
1	DI water, 2.5	MBAA, 0.46	2	DI Water, 1.5	PAA+0.01MBAA[a]
1	DI water, 2.5	MBAA, 0.046	2	DI Water, 1.5	PAA+0.001MBAA[a]

1	30 mg/mL lignin particle, 2.5	MBAA, 4.6	2	DI Water, 1.5	PAA+0.1MBAA+3LG[a]
1	30 mg/mL lignin particle, 2.5	MBAA, 0.46	2	DI Water, 1.5	PAA+0.01MBAA+3LG[a]
1	30 mg/mL lignin particle, 2.5	MBAA, 0.046	2	DI Water, 1.5	PAA+0.001MBAA+3LG[a]
1	DI water, 2.5	AAm, 500	-	5 w/v% CA/Water, 1.5	PAAm
1	5 mg/mL lignin particle, 2.5	AAm, 500	-	5 w/v% CA/Water, 1.5	PAAm+0.5LG
1	10 mg/mL lignin particle, 2.5	AAm, 500	-	5 w/v% CA/Water, 1.5	PAAm+1LG
1	20 mg/mL lignin particle, 2.5	AAm, 500	-	5 w/v% CA/Water, 1.5	PAAm+2LG

[a] Numbers including 0.1, 0.01 and 0.001 before term “MBAA” stand for the mole ratio of MBAA to monomer AA in the hydrogel precursor solution.

References

1. D. Gan, W. Xing, L. Jiang, J. Fang, C. Zhao, F. Ren, L. Fang, K. Wang and X. Lu, *Nat. Commun.*, 2019, **10**, 1-10.
2. W. Luo, L. Liu, G. Qi, F. Yang, X. Shi and X. Zhao, *Appl. Environ. Microbiol.*, 2019, **85**, e03128-03118.
3. X.-G. Sun, Y. Fang, X. Jiang, K. Yoshii, T. Tsuda and S. Dai, *Chem. Commun.*, 2016, **52**, 292-295.
4. R. Coşkun and A. Delibaş, *Polym. Bull. (Berlin)*, 2012, **68**, 1889-1903.
5. K. Somord, K. Somord, O. Suwantong, C. Thanomsilp, T. Peijs and N. Soykeabkaew, *Nanocomposites*, 2018, **4**, 102-111.
6. G. Yu, A. Cao and C. M. Lieber, *Nat. Nanotechnol.*, 2007, **2**, 372-377.
7. Q. Li, F. Bai, J. Sun, X. Zhou, W. Yuan, J. Lin, K.-Q. Zhang, G. Li and Z. Liu, *Nanoscale*, 2023.
8. X. Yang, L. Li, S. Wang, Q. Lu, Y. Bai, F. Sun, T. Li, Y. Li, Z. Wang and Y. Zhao, *Adv. Electron. Mater.*, 2020, **6**, 2000306.
9. W. Chen and L. Yan, *Advanced Materials (Deerfield Beach, Fla.)*, 2012, **24**, 6229-6233.
10. X. W. Zhongxue Bai, Manhui Zheng, Ouyang Yue, Mengchen Huang, Xiaoliang Zou, Boqiang Cui, Long Xie, Shuyin Dong, Jiaojiao Shang, Guidong Gong, Anna M. Blocki, Junling Guo, Xinhua Liu, *Adv. Funct. Mater.*, 2023, DOI: 10.1002/adfm.202212856, 202212856.
11. X. Fu, J. Li, C. Tang, S. Xie, X. Sun, B. Wang and H. Peng, *Adv. Funct. Mater.*, 2021, **31**, 2008355.
12. Z. Wu, S. Chen, R. Wu, N. Sheng, M. Zhang, P. Ji and H. Wang, *Chem. Eng. J.*, 2020, **391**, 123527.
13. Y. Tian, X. Wei, Z. J. Wang, P. Pan, F. Li, D. Ling, Z. L. Wu and Q. Zheng, *ACS Appl. Mater. Interfaces*, 2017, **9**, 34349-34355.
14. S. Singamaneni, M. E. McConney and V. V. Tsukruk, *Adv. Mater.*, 2010, **22**, 1263-1268.
15. Z. Yang, Y. He, S. Liao, Y. Ma, X. Tao and Y. Wang, *Sci. Adv.*, 2021, **7**, eabf9117.
16. J. L. Lilly, G. Romero, W. Xu, H. Y. Shin and B. J. Berron, *Biomacromol.*, 2015, **16**, 541-549.
17. M. He, Q. Wang, Z. Shi, Y. Xie, W. Zhao and C. Zhao, *Colloid Surf. B*, 2017, **158**, 518-526.
18. G. Parada, Y. Yu, W. Riley, S. Lojovich, D. Tshikudi, Q. Ling, Y. Zhang, J. Wang, L. Ling and Y. Yang, *Adv. Healthc. Mater.*, 2020, **9**, 2001116.
19. Y. Yu, H. Yuk, G. A. Parada, Y. Wu, X. Liu, C. S. Nabzdyk, K. Youcef-Toumi, J. Zang and X. Zhao, *Adv. Mater.*, 2019, **31**, 1807101.
20. V. Kozlovskaya, E. Kharlampieva, M. L. Mansfield and S. A. Sukhishvili, *Chem. Mater.*, 2006, **18**, 328-336.
21. Y. Xia, Z. Wang, L.-Y. Chen, S.-W. Xiong, P. Zhang, P.-G. Fu and J.-G. Gai, *Desalination*, 2020, **488**, 114510.
22. S. Gao, Y. Zhu, J. Wang, F. Zhang, J. Li and J. Jin, *Adv. Funct. Mater.*, 2018, **28**, 1801944.
23. S. Kim, W. Choi, D. J. Kim, H. S. Jung, D.-H. Kim, S.-H. Kim and S.-G. Park, *Nanoscale*, 2020, **12**, 12942-12949.
24. L. Witzdam, Y. L. Meurer, M. Garay-Sarmiento, M. Vorobii, D. Söder, J. Quandt, T. Haraszti and C. Rodriguez-Emmenegger, *Macromol. Biosci.*, 2022, **22**, 2200025.
25. Y. Dong, E. M. Akinoglu, H. Zhang, F. Maasoumi, J. Zhou and P. Mulvaney, *Adv. Funct. Mater.*, 2019, **29**, 1904290.
26. L. Wang, H. Liu, F. Zhang, G. Li and S. Wang, *Small*, 2016, **12**, 4697-4701.
27. J. Liu, S. Lin, X. Liu, Z. Qin, Y. Yang, J. Zang and X. Zhao, *Nat. Commun.*, 2020, **11**,

1071.
28. Q. Wang, X. Pan, C. Lin, X. Ma, S. Cao and Y. Ni, *Chem. Eng. J.*, 2020, **396**, 125341.
29. L. Peng, L. Chang, M. Si, J. Lin, Y. Wei, S. Wang, H. Liu, B. Han and L. Jiang, *ACS Appl. Mater. Interfaces*, 2020, **12**, 9718-9725.
30. M. Qin, M. Sun, R. Bai, Y. Mao, X. Qian, D. Sikka, Y. Zhao, H. J. Qi, Z. Suo and X. He, *Adv. Mater.*, 2018, **30**, 1800468.
31. M. Sun, R. Bai, X. Yang, J. Song, M. Qin, Z. Suo and X. He, *Adv. Mater.*, 2018, **30**, 1804916.
32. X. Yao, J. Liu, C. Yang, X. Yang, J. Wei, Y. Xia, X. Gong and Z. Suo, *Adv. Mater.*, 2019, **31**, 1903062.
33. Z. Bai, K. Jia, C. Liu, L. Wang, G. Lin, Y. Huang, S. Liu and X. Liu, *Adv. Funct. Mater.*, 2021, **31**, 2104701.
34. J. Yang, B. Xue, Y. Zhou, M. Qin, W. Wang and Y. Cao, *Adv. Mater. Technol.*, 2021, **6**, 2000911.
35. Y. Liu, L. Wang, M. Zhang, D. Tu, X. Mao and Y. Liao, *IEEE Photon. Technol. Lett.*, 2007, **19**, 880-882.
36. H. Huang, T. Kowalewski, E. E. Remsen, R. Gertzmann and K. L. Wooley, *J. Am. Chem. Soc.*, 1997, **119**, 11653-11659.
37. D. Qin, Z. Liu, H. Bai, X. Song, Z. Li and D. D. Sun, *J. Membr. Sci.*, 2019, **592**, 117370.
38. W. Wang, P. Lu, Y. Fan, L. Tian, S. Niu, J. Zhao and L. Ren, *Chem. Eng. J.*, 2019, **378**, 122173.
39. D. Silva, H. C. de Sousa, M. H. Gil, L. F. Santos, G. M. Moutinho, M. Salema-Oom, C. Alvarez-Lorenzo, A. P. Serro and B. Saramago, *Int. J. Pharm.*, 2020, **585**, 119506.
40. J. Choi, M. Hua, S. Y. Lee, W. Jo, C. Y. Lo, S. H. Kim, H. T. Kim and X. He, *Adv. Opt. Mater.*, 2020, **8**, 1901259.
41. S. Cheng, Z. Lou, L. Zhang, H. Guo, Z. Wang, C. Guo, K. Fukuda, S. Ma, G. Wang and T. Someya, *Adv. Mater.*, 2023, **35**, 2206793.
42. Y. Gao, X. Han, J. Chen, Y. Pan, M. Yang, L. Lu, J. Yang, Z. Suo and T. Lu, *Proc. Natl. Acad. Sci.*, 2021, **118**, e2103457118.
43. Z. Wu, H. Ding, K. Tao, Y. Wei, X. Gui, W. Shi, X. Xie and J. Wu, *ACS Appl. Mater. Interfaces*, 2021, **13**, 21854-21864.